

Supporting Information

A five-fold interpenetrated metal-organic framework showing large variation in thermal expansion behaviour owing to dramatic structural transformation upon dehydration-rehydration

Himanshu Aggarwal,[‡] Raj Kumar Das,[‡] Emile R. Engel and Leonard J. Barbour*

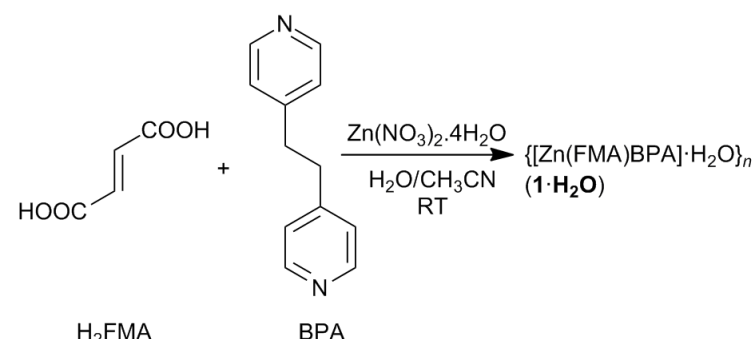
Department of Chemistry and Polymer Science, University of Stellenbosch, Matieland 7602,
Stellenbosch, South Africa

Synthesis

All chemicals and solvent used in these experiments were purchased from Aldrich and used without any further purification.

Synthesis of $\{[\text{Zn}(\text{FMA})(\text{BPA})]\cdot\text{H}_2\text{O}\}_n$ (**1**· H_2O)

8.1 mg (0.07 mmol) of fumaric acid and 21.2 mg (0.07 mmol) of $\text{Zn}(\text{NO}_3)_2\cdot 4\text{H}_2\text{O}$ were dissolved in 4 ml of H_2O . A 4 ml acetonitrile solution of 1,2-bis(4-pyridyl)ethane (37.2 mg, 0.2 mmol) was then layered carefully onto the aqueous solution containing fumaric acid and $\text{Zn}(\text{NO}_3)_2\cdot 6\text{H}_2\text{O}$. Single crystals of **1**· H_2O suitable for X-ray analysis were obtained in one week.



Scheme S1. Synthetic scheme for **1**· H_2O .

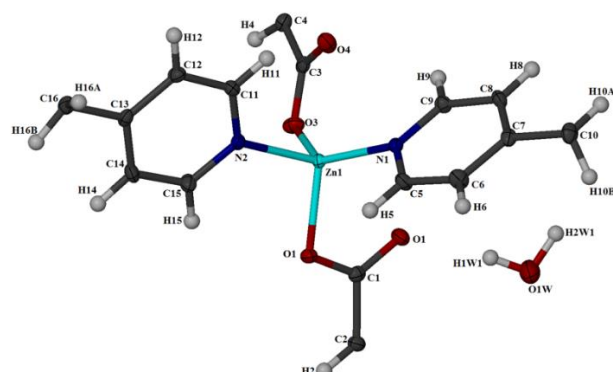


Figure S1 Asymmetric unit showing Zn(II) in a tetrahedral coordination environment (thermal ellipsoid plot). The $\text{Zn}\cdots\text{O}$ distances for the non-coordinated oxygen atoms are greater than 2.5 Å, confirming absence of formal Zn-O coordination bond in these two cases.¹

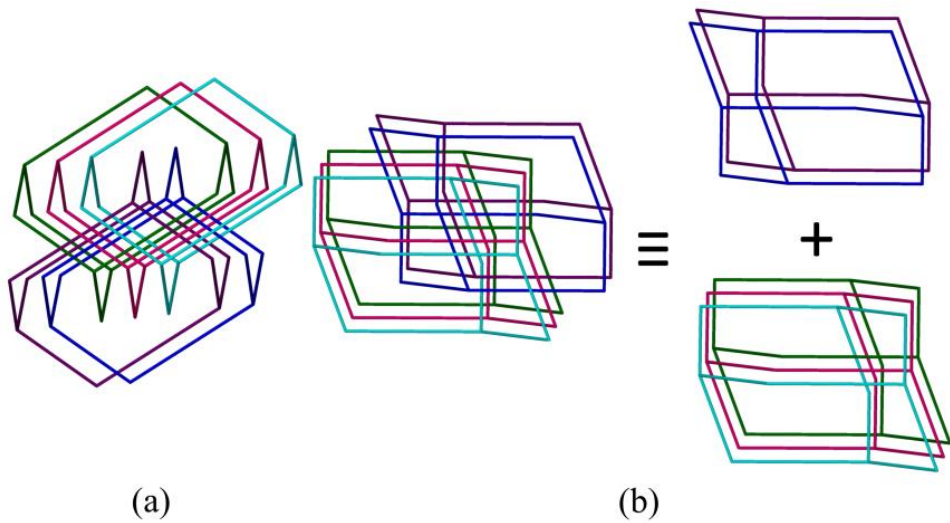


Figure S2 (a) Perspective view of 5-fold interpenetration and (b) Graphical rendition of the [2+3]-fold interpenetration in **1·H₂O**

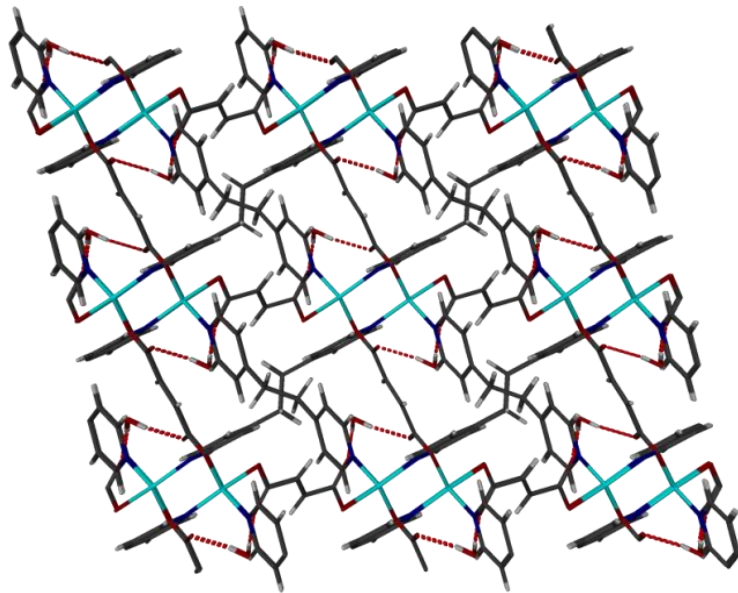


Figure S3 Perspective showing the crystal packing in **1·H₂O**

Single Crystal X-ray Diffraction (SCXRD)

Single crystal X-ray diffraction data were collected on a Bruker APEX-II Quasar CCD area-detector diffractometer equipped with an Oxford Cryosystems Cryostream 700Plus cryostat. A multilayer monochromator with Mo K_α radiation ($\lambda = 0.71073 \text{ \AA}$) from an Incoatec I_μS microsource was used.

Data reduction was carried out by means of standard procedures using the Bruker software package SAINT² and absorption corrections and the correction of other systematic errors were performed using SADABS.³ The structures were solved by direct methods using SHELXS-97 and refined using SHELXL-97.⁴ X-Seed⁵ was used as the graphical interface for the SHELX program suite. Hydrogen atoms were placed in calculated positions using riding models.

Table S1 Crystallographic details for 1·H₂O

Identification code	100K	120K	140K	160K	180K
Empirical formula	C ₁₆ H ₁₆ N ₂ O ₅ Zn	C ₁₆ H ₁₆ N ₂ O ₅ Zn	C ₁₆ H ₁₆ N ₂ O ₅ Zn	C ₁₆ H ₁₆ N ₂ O ₅ Zn	C ₁₆ H ₁₆ N ₂ O ₅ Zn
Formula weight	381.68	381.68	381.68	381.68	381.68
Temperature/K	100(2)	120(2)	140(2)	160(2)	180(2)
Crystal system	Triclinic	Triclinic	Triclinic	Triclinic	Triclinic
Space group	P $\bar{1}$				
<i>a</i> /Å	8.3664(2)	8.3788(2)	8.3909(2)	8.4043(3)	8.4179(2)
<i>b</i> /Å	9.2360(3)	9.2243(2)	9.2121(2)	9.1990(3)	9.1829(2)
<i>c</i> /Å	11.1630(3)	11.1762(3)	11.1901(3)	11.2066(4)	11.2234(3)
α°	90.482(2)	90.546(2)	90.620(2)	90.703(2)	90.807(2)
β°	110.353(2)	110.3970(10)	110.447(2)	110.501(2)	110.5540(10)
γ°	100.7260(10)	100.5640(10)	100.3850(10)	100.187(2)	99.9510(10)
Volume/Å ³	792.10(4)	793.38(3)	794.64(3)	796.14(5)	797.49(3)
<i>Z</i>	2	2	2	2	2
$\rho_{\text{calc}}/\text{cm}^3$	1.600	1.598	1.595	1.592	1.589
μ/mm^{-1}	1.580	1.577	1.574	1.572	1.569
F(000)	392	392	392	392	392
Crystal size/mm ³	0.819 × 0.220 × 0.130	0.821 × 0.220 × 0.130	0.823 × 0.221 × 0.130	0.826 × 0.222 × 0.129	0.827 × 0.223 × 0.129
Radiation	MoK α (λ = 0.71073)				
θ range for data collection/ $^{\circ}$	1.95 to 26.04	1.95 to 26.06	1.95 to 26.05	1.95 to 26.05	1.94 to 26.06
Index ranges	-10 ≤ <i>h</i> ≤ 10, -11 ≤ <i>k</i> ≤ 11, -13 ≤ <i>l</i> ≤ 13	-10 ≤ <i>h</i> ≤ 10, -11 ≤ <i>k</i> ≤ 11, -13 ≤ <i>l</i> ≤ 13	-10 ≤ <i>h</i> ≤ 10, -11 ≤ <i>k</i> ≤ 11, -13 ≤ <i>l</i> ≤ 13	-10 ≤ <i>h</i> ≤ 10, -11 ≤ <i>k</i> ≤ 11, -13 ≤ <i>l</i> ≤ 13	-10 ≤ <i>h</i> ≤ 10, -11 ≤ <i>k</i> ≤ 11, -13 ≤ <i>l</i> ≤ 13
Reflections collected	10510	10532	10570	10591	10632
Independent reflections	3121 [R _{int} = 0.0196, R _{sigma} = 0.0178]	3128 [R _{int} = 0.0197, R _{sigma} = 0.0182]	3131 [R _{int} = 0.0195, R _{sigma} = 0.0182]	3141 [R _{int} = 0.0200, R _{sigma} = 0.0186]	3155 [R _{int} = 0.0204, R _{sigma} = 0.0193]
Data/restraints/parameters	3121/0/219	3128/0/222	3131/0/222	3141/0/219	3155/0/222
Goodness-of-fit on F ²	1.042	1.031	1.029	1.048	1.049
Final R indexes [<i>I</i> >=2σ] (I)	R ₁ = 0.0217, wR ₂ = 0.0535	R ₁ = 0.0221, wR ₂ = 0.0550	R ₁ = 0.0231, wR ₂ = 0.0581	R ₁ = 0.0238, wR ₂ = 0.0605	R ₁ = 0.0254, wR ₂ = 0.0656
Final R indexes [all data]	R ₁ = 0.0227, wR ₂ = 0.0540	R ₁ = 0.0231, wR ₂ = 0.0556	R ₁ = 0.0244, wR ₂ = 0.0588	R ₁ = 0.0252, wR ₂ = 0.0613	R ₁ = 0.0271, wR ₂ = 0.0665
Largest diff. peak/hole / e Å ⁻³	0.395/-0.278	0.496/-0.314	0.590/-0.386	0.634/-0.391	0.742/-0.414
Mosaicity/ $^{\circ}$	0.43	0.42	0.42	0.42	0.42

Identification code	200K	220K	240K	100K-R
Empirical formula	C ₁₆ H ₁₆ N ₂ O ₅ Zn	C ₁₆ H ₁₆ N ₂ O ₅ Zn	C ₁₆ H ₁₆ N ₂ O ₅ Zn	C ₁₆ H ₁₆ N ₂ O ₅ Zn
Formula weight	381.68	381.68	381.68	381.68
Temperature/K	200(2)	220(2)	2400(2)	100(2)
Crystal system	Triclinic	Triclinic	Triclinic	Triclinic
Space group	P $\bar{1}$	P $\bar{1}$	P $\bar{1}$	P $\bar{1}$
<i>a</i> /Å	8.4318(2)	8.4474(2)	8.4619(2)	8.3703(2)
<i>b</i> /Å	9.1634(2)	9.1453(2)	9.1264(2)	9.2341(2)
<i>c</i> /Å	11.2411(3)	11.2631(3)	11.2843(3)	11.1634(3)
α°	90.9330(10)	91.0590(10)	91.177(2)	90.4570(10)
β°	110.6020(10)	110.6610(10)	110.7170(10)	110.3660(10)
γ°	99.6860(10)	99.3900(10)	99.0880(10)	100.7520(10)
Volume/Å ³	798.71(3)	800.52(3)	802.11(3)	792.21(3)
<i>Z</i>	2	2	2	2
$\rho_{\text{calc}}/\text{cm}^3$	1.587	1.583	1.580	1.600
μ/mm^{-1}	1.566	1.563	1.560	1.579
F(000)	392	392	392	392
Crystal size/mm ³	0.829 × 0.224 × 0.128	0.832 × 0.224 × 0.128	0.833 × 0.225 × 0.128	0.819 × 0.220 × 0.130
Radiation	MoK α (λ = 0.71073)	MoK α (λ = 0.71073)	MoK α (λ = 0.71073)	MoK α (λ = 0.71073)
θ range for data collection/ $^{\circ}$	1.94 to 26.08	1.94 to 26.02	1.94 to 26.06	2.13 to 25.97
Index ranges	-10 ≤ <i>h</i> ≤ 10, -11 ≤ <i>k</i> ≤ 11, -13 ≤ <i>l</i> ≤ 13	-10 ≤ <i>h</i> ≤ 10, -11 ≤ <i>k</i> ≤ 11, -13 ≤ <i>l</i> ≤ 13	-10 ≤ <i>h</i> ≤ 10, -11 ≤ <i>k</i> ≤ 11, -13 ≤ <i>l</i> ≤ 13	-9 ≤ <i>h</i> ≤ 10, -11 ≤ <i>k</i> ≤ 11, -13 ≤ <i>l</i> ≤ 13

Reflections collected	10672	10573	10647	10622
Independent reflections	3163 [$R_{\text{int}} = 0.0213$, $R_{\text{sigma}} = 0.0197$]	3144 [$R_{\text{int}} = 0.0214$, $R_{\text{sigma}} = 0.0202$]	3165 [$R_{\text{int}} = 0.0219$, $R_{\text{sigma}} = 0.0204$]	3120 [$R_{\text{int}} = 0.0180$, $R_{\text{sigma}} = 0.0167$]
Data/restraints/parameters	3163/0/222	3144/0/222	3165/2/219	3120/0/219
Goodness-of-fit on F^2	1.035	1.060	1.026	1.032
Final R indexes [$I \geq 2\sigma (I)$]	$R_1 = 0.0266$, $wR_2 = 0.0692$	$R_1 = 0.0286$, $wR_2 = 0.0733$	$R_1 = 0.0306$, $wR_2 = 0.0771$	$R_1 = 0.0217$, $wR_2 = 0.0556$
Final R indexes [all data]	$R_1 = 0.0285$, $wR_2 = 0.0682$	$R_1 = 0.0306$, $wR_2 = 0.0745$	$R_1 = 0.0329$, $wR_2 = 0.0787$	$R_1 = 0.0225$, $wR_2 = 0.0560$
Largest diff. peak/hole / e Å ⁻³	0.737/-0.470	0.758/-0.478	0.787/-0.546	0.424/-0.269
Mosaicity/°	0.41	0.42	0.41	0.43

Table S2 Unit cell axes at variable temperatures for **1·H₂O**.

T (K)	a (Å)	St. dev.*	b (Å)	St. dev.*	c (Å)	St. dev. *	Crystal mosaicity
100	8.3664	0.0002	9.2360	0.0003	11.1630	0.0003	0.43°
120	8.3788	0.0002	9.2243	0.0002	11.1762	0.0003	0.42°
140	8.3909	0.0002	9.2121	0.0002	11.1901	0.0003	0.42°
160	8.4043	0.0003	9.1990	0.0003	11.2066	0.0004	0.42°
180	8.4179	0.0002	9.1829	0.0002	11.2234	0.0003	0.42°
200	8.4318	0.0002	9.1634	0.0002	11.2411	0.0003	0.41°
220	8.4474	0.0002	9.1453	0.0002	11.2631	0.0003	0.42°
240	8.4619	0.0002	9.1264	0.0002	11.2843	0.0003	0.41°
100-R	8.3703	0.0002	9.2341	0.0002	11.1634	0.0003	0.43°

*Standard deviation calculated from unit cell refinement using the Apex II software suite.

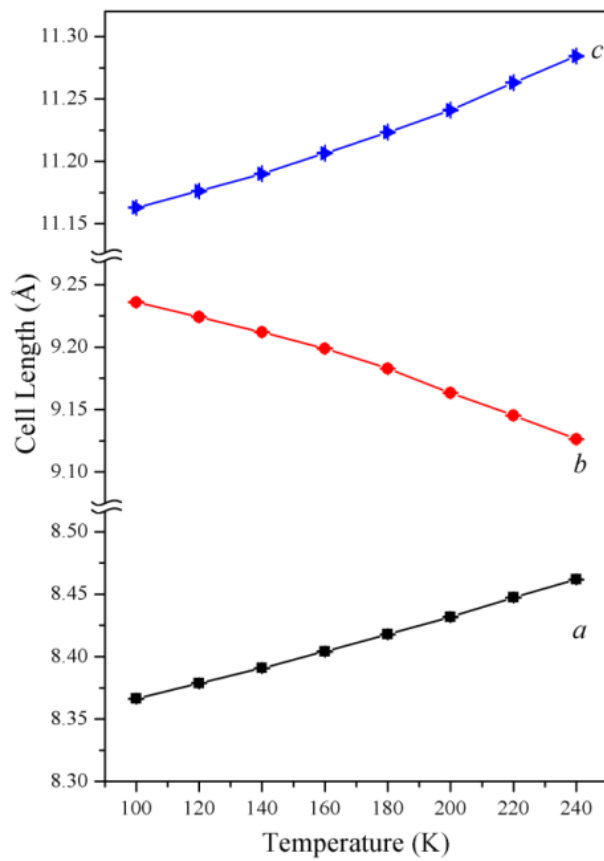
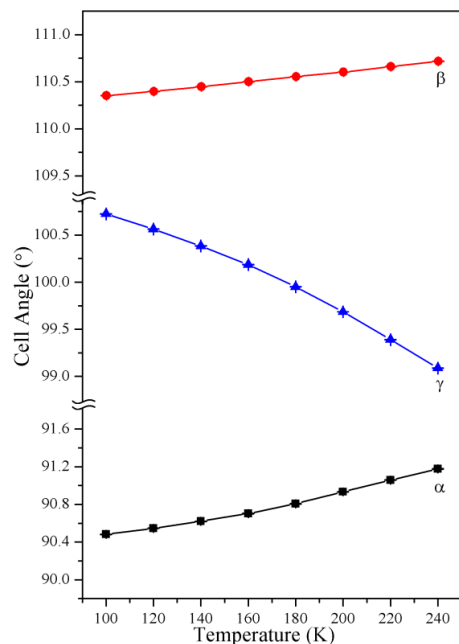
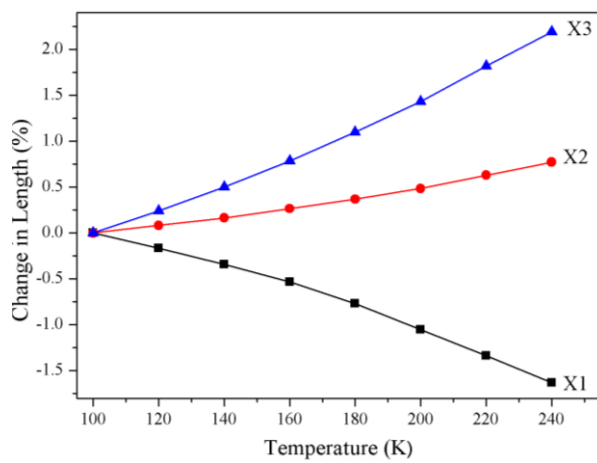


Figure S4 Variation of unit cell axes of **1·H₂O** (including error bars) with temperature.

Table S3 Unit cell angles and volume at variable temperatures for **1·H₂O**.

T (K)	α (°)	St. dev.*	β (°)	St. dev.*	γ (°)	St. dev. *	V(Å ³)	St. dev. *	Crystal mosaicity
100	90.482	0.002	110.353	0.002	100.726	0.002	792.1	0.04	0.43°
120	90.546	0.002	110.397	0.001	100.564	0.001	793.38	0.03	0.42°
140	90.62	0.002	110.447	0.002	100.385	0.001	794.64	0.03	0.42°
160	90.703	0.002	110.501	0.002	100.187	0.002	796.14	0.05	0.42°
180	90.807	0.002	110.554	0.001	99.951	0.001	797.49	0.03	0.42°
200	90.933	0.001	110.602	0.001	99.686	0.001	798.71	0.03	0.41°
220	91.059	0.001	110.661	0.001	99.39	0.001	800.52	0.03	0.42°
240	91.177	0.002	110.717	0.001	99.088	0.001	802.11	0.03	0.41°
100-R	90.457	0.001	110.366	0.001	100.752	0.001	792.21	0.03	0.43°

*Standard deviation calculated from unit cell refinement using the Apex II software suite.

**Figure S5** Variation of unit cell angles of **1·H₂O** (including error bars) with temperature**Fig. S6** Plot of changes in principal axis lengths with increasing temperature for **1·H₂O**

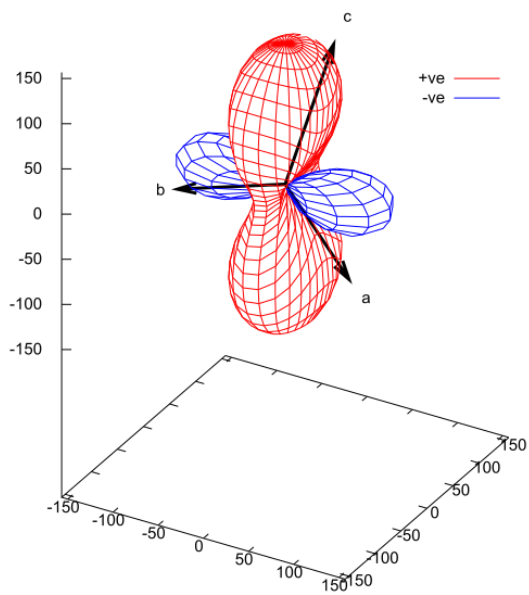


Figure S7 PASCal expansivity tensor plot for **1·H₂O**

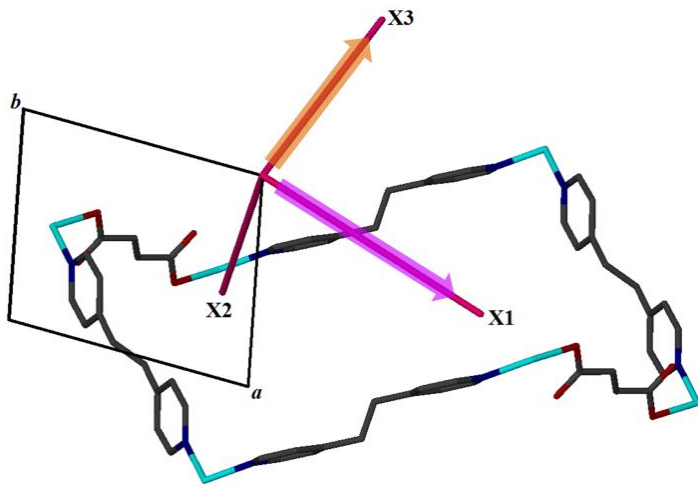


Figure S8 The orthogonal directions of the principal axes, X1 (NTE) and X3 (PTE) projected onto the crystallographic *ab* plane of **1·H₂O**.

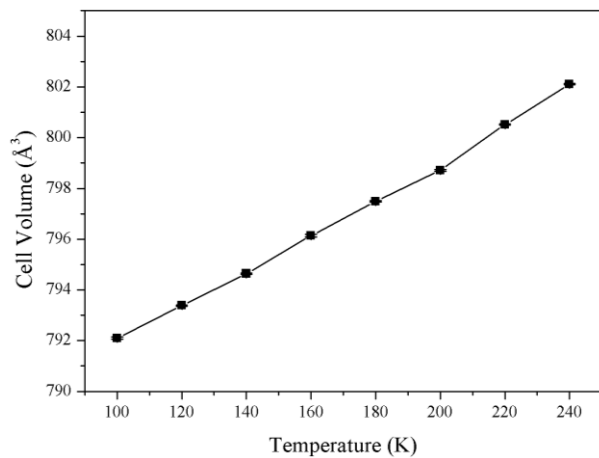


Figure S9 Variation of unit cell volume of **1·H₂O** (including error bars) with temperature.

Table S4 Selected bond angles at variable temperatures for **1·H₂O**.

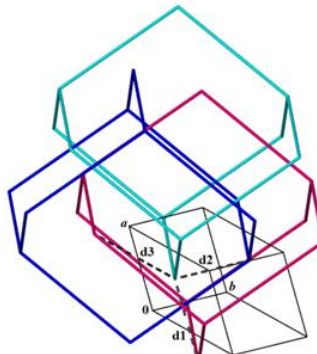
T (K)	O1–Zn1–N1 (°)	O1–Zn1–O3 (°)	O3–Zn1–N1 (°)	N1–Zn1–N2 (°)	O3–Zn1–N2 (°)	O1–Zn1–N2 (°)
100	108.34(5)	103.31(5)	132.68(5)	106.66(5)	101.46(5)	99.78(5)
120	108.46(5)	103.30(5)	132.83(5)	106.44(6)	101.43(5)	99.69(5)
140	108.50(6)	103.36(5)	132.96(6)	106.27(6)	101.40(6)	99.58(5)
160	108.59(6)	103.43(6)	133.08(6)	106.09(6)	101.37(6)	99.40(6)
180	108.69(6)	103.42(6)	133.40(7)	105.73(6)	101.35(6)	99.22(6)
200	108.75(6)	103.46(7)	133.66(7)	105.42(7)	101.33(7)	99.01(6)
220	108.81(7)	103.42(7)	134.10(8)	105.06(7)	101.33(8)	98.69(7)
240	108.84(8)	103.38(8)	134.60(8)	104.74(8)	101.15(8)	98.41(7)

Table S5 List of selected non-bonding distances (in Å) within a single diamondoid network at variable temperatures for **1·H₂O**.

T (K)	Zn1…Zn2 [0 2 1]	Zn2…Zn3 [-1 2 0]	Zn1…Zn3 [1 0 -1]
100	21.5025(7)	18.8065(6)	16.1113(5)
120	21.4786(6)	18.8116(5)	16.1365(4)
140	21.4524(6)	18.8182(5)	16.1626(5)
160	21.4246(7)	18.8262(7)	16.1923(6)
180	21.3883(6)	18.8343(5)	16.2224(5)
200	21.3430(5)	18.8406(5)	16.2530(5)
220	21.3023(6)	18.8544(5)	16.2898(5)
240	21.2612(6)	18.8673(5)	16.3247(5)

Table S6 List of selected inter diamondoid network distances at variable temperatures for **1·H₂O**.

T (K)	d1 (Å)	d2 (Å)	d3 (Å)
100	8.3664(3)	9.2360(4)	11.1630(4)
120	8.3788(3)	9.2243(3)	11.1762(4)
140	8.3909(3)	9.2121(3)	11.1901(4)
160	8.4043(5)	9.1990(4)	11.2066(5)
180	8.4179(4)	9.1829(3)	11.2234(5)
200	8.4318(4)	9.1634(3)	11.2411(5)
220	8.4474(4)	9.1453(4)	11.2631(5)
240	8.4619(4)	9.1264(4)	11.2843(5)

**Table S7.** List of O–H…O hydrogen bonding interactions in **1·H₂O** in the temperature range 100 K and 240 K.

T(K)	O1W–H2W1…O5				O1W–H1W1…O3			
	d(O–H)	d(H…O)	d(O…O)	<OHO	d(O–H)	d(H…O)	d(O…O)	<OHO
100	0.887(2)	1.936(1)	2.818(2)	171.8(1)	0.962(2)	1.939(1)	2.889(2)	168.7(1)
120	0.924(2)	1.897(1)	2.816 (3)	173.1(1)	0.940(2)	1.952(1)	2.888(2)	175.0(1)
140	0.965(2)	1.856(1)	2.812(3)	170.1(1)	0.953(2)	1.940(1)	2.889(291)	173.6(1)
160	0.947(2)	1.871(2)	2.812(3)	171.6(1)	0.963(2)	1.929(1)	2.886(2)	172.1(1)
180	0.96(5)	1.86(5)	2.810(3)	172(4)	0.989(2)	1.898(1)	2.884(2)	166.4(1)
200	0.95(5)	1.87(5)	2.806(4)	169(4)	0.961(2)	1.928(2)	2.881(3)	171.2(1)
220	0.98(7)	1.83(7)	2.803(4)	171(5)	1.007(3)	1.871(2)	2.877(3)	171.4(2)
240	1.020(4)	1.775(2)	2.794(5)	175.5(2)	0.932(3)	1.943(2)	2.872(4)	171.1(2)

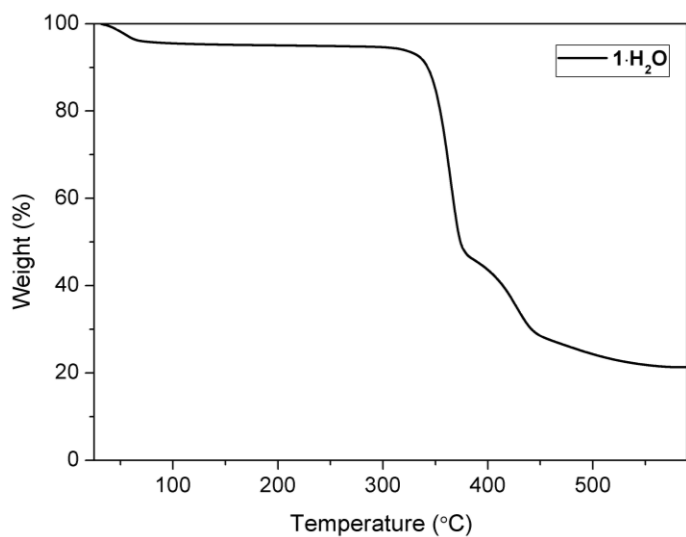


Figure S10 Thermogravimetric analysis of $\mathbf{1}\cdot\text{H}_2\text{O}$

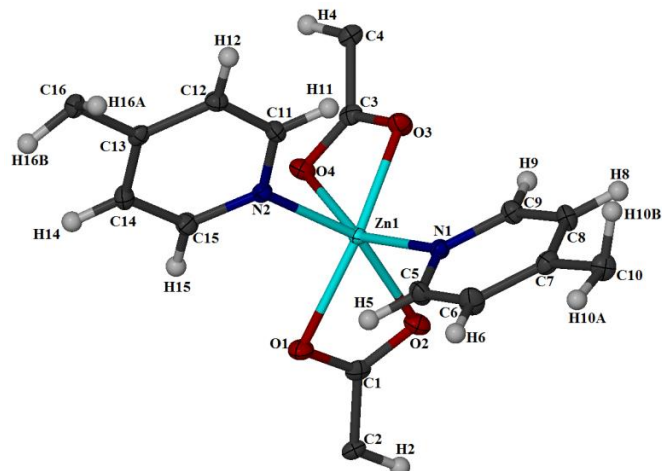


Figure S11 Thermal ellipsoid plot of the asymmetric unit of $\mathbf{1}$.

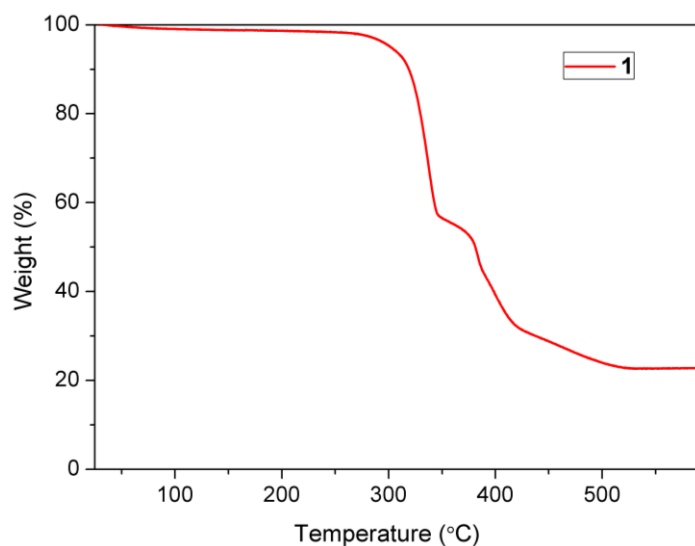


Figure S12 Thermogravimetric analysis of $\mathbf{1}$

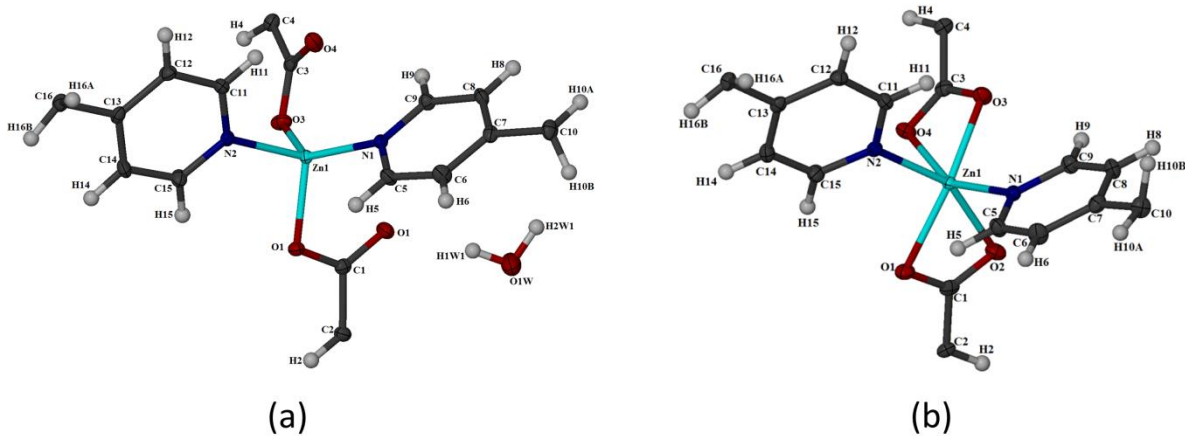


Figure S13 Thermal ellipsoid plots of the asymmetric units of (a) **1**·H₂O and (b) **1**.

Table S8 Crystallographic details for **1**

The compound **1** is devoid of any water molecules and we therefore recorded the data up to a temperature of 298 K. However for direct comparison of the thermal expansion behavior of **1**·H₂O and **1**, we only used the data to 240 K.

Identification code	100K	120K	140K	160K	180K	200K
Empirical formula	C ₁₆ H ₁₄ N ₂ O ₄ Zn	C ₁₆ H ₁₄ N ₂ O ₄ Zn	C ₁₆ H ₁₄ N ₂ O ₄ Zn	C ₁₆ H ₁₄ N ₂ O ₄ Zn	C ₁₆ H ₁₄ N ₂ O ₄ Zn	C ₁₆ H ₁₄ N ₂ O ₄ Zn
Formula weight	363.66	363.66	363.66	363.66	363.66	363.66
Temperature/K	100(2)	120(2)	140(2)	160(2)	180(2)	180(2)
Crystal system	Triclinic	Triclinic	Triclinic	Triclinic	Triclinic	Triclinic
Space group	P $\bar{1}$					
<i>a</i> /Å	8.1663(2)	8.16960(10)	8.17180(10)	8.17420(10)	8.17690(10)	8.17940(10)
<i>b</i> /Å	8.8936(2)	8.8871(2)	8.8796(2)	8.8724(2)	8.86560(10)	8.85960(10)
<i>c</i> /Å	11.2600(2)	11.2748(2)	11.2884(2)	11.3032(2)	11.3207(2)	11.3396(2)
α /°	92.3050(10)	92.3120(10)	92.3220(10)	92.3430(10)	92.3610(10)	92.3730(10)
β /°	107.6700(10)	107.6620(10)	107.6610(10)	107.6650(10)	107.6670(10)	107.6690(10)
γ /°	95.6650(10)	95.5990(10)	95.5300(10)	95.4570(10)	95.3830(10)	95.3090(10)
Volume/Å ³	773.27(3)	774.17(2)	774.77(2)	775.46(2)	776.416(19)	776.476(19)
Z	2	2	2	2	2	2
$\rho_{\text{calc}}/\text{cm}^3$	1.562	1.560	1.559	1.557	1.556	1.553
μ/mm^{-1}	1.609	1.607	1.606	1.605	1.603	1.603
F(000)	372	372	372	372	372	372
Crystal size/mm ³	0.246 × 0.131 × 0.086	0.247 × 0.131 × 0.086	0.247 × 0.131 × 0.086	0.247 × 0.131 × 0.086	0.248 × 0.131 × 0.086	0.248 × 0.131 × 0.085
Radiation	MoKα ($\lambda = 0.71073$)					
θ range for data collection/°	1.90 to 26.13	1.90 to 26.12	1.90 to 26.15	1.90 to 26.15	1.89 to 26.01	1.89 to 26.12
Index ranges	-10 ≤ <i>h</i> ≤ 9, -11 ≤ <i>k</i> ≤ 10, -13 ≤ <i>l</i> ≤ 13	-10 ≤ <i>h</i> ≤ 9, -11 ≤ <i>k</i> ≤ 10, -13 ≤ <i>l</i> ≤ 13	-10 ≤ <i>h</i> ≤ 9, -10 ≤ <i>k</i> ≤ 10, -13 ≤ <i>l</i> ≤ 13	-10 ≤ <i>h</i> ≤ 9, -10 ≤ <i>k</i> ≤ 10, -13 ≤ <i>l</i> ≤ 14	-10 ≤ <i>h</i> ≤ 9, -10 ≤ <i>k</i> ≤ 10, -13 ≤ <i>l</i> ≤ 13	-10 ≤ <i>h</i> ≤ 9, -10 ≤ <i>k</i> ≤ 10, -14 ≤ <i>l</i> ≤ 14
Reflections collected	10666	10666	10674	10706	10633	10738
Independent reflections	3070 [R _{int} = 0.0253, R _{sigma} = 0.0240]	3070 [R _{int} = 0.0249, R _{sigma} = 0.0238]	3076 [R _{int} = 0.0228, R _{sigma} = 0.0217]	3916 [R _{int} = 0.0235, R _{sigma} = 0.0223]	3044 [R _{int} = 0.0231, R _{sigma} = 0.0218]	3087 [R _{int} = 0.0234, R _{sigma} = 0.0220]
Data/restraints/parameters	3070/0/208	3070/0/208	3076/0/208	3086/0/208	3044/0/208	3087/0/208
Goodness-of-fit on F ²	1.059	1.046	1.040	1.060	1.033	1.067
Final R indexes [<i>I</i> >=2σ (<i>I</i>)]	R ₁ = 0.0229, wR ₂ = 0.0538	R ₁ = 0.0227, wR ₂ = 0.0548	R ₁ = 0.0224, wR ₂ = 0.0535	R ₁ = 0.0222, wR ₂ = 0.0536	R ₁ = 0.0225, wR ₂ = 0.0543	R ₁ = 0.0229, wR ₂ = 0.0555
Final R indexes [all data]	R ₁ = 0.0246, wR ₂ = 0.0545	R ₁ = 0.0247, wR ₂ = 0.0556	R ₁ = 0.0242, wR ₂ = 0.0542	R ₁ = 0.0240, wR ₂ = 0.0543	R ₁ = 0.0246, wR ₂ = 0.0552	R ₁ = 0.0253, wR ₂ = 0.0565
Largest diff. peak/hole / e Å ⁻³	0.327/-0.260	0.323/-0.228	0.303/-0.227	0.288/-0.198	0.291/-0.202	0.320/-0.221
Mosaicity/°	0.39	0.39	0.40	0.40	0.40	0.39

Identification code	220K	240K	260K	280 K	298 K	100 K-R
Empirical formula	C ₁₆ H ₁₄ N ₂ O ₄ Zn	C ₁₆ H ₁₄ N ₂ O ₄ Zn	C ₁₆ H ₁₄ N ₂ O ₄ Zn	C ₁₆ H ₁₄ N ₂ O ₄ Zn	C ₁₆ H ₁₄ N ₂ O ₄ Zn	C ₁₆ H ₁₄ N ₂ O ₄ Zn
Formula weight	363.66	363.66	363.66	363.66	363.66	363.66
Temperature/K	220(2)	240(2)	260(2)	280(2)	180(2)	180(2)
Crystal system	Triclinic	Triclinic	Triclinic	Triclinic	Triclinic	Triclinic
Space group	P $\bar{1}$					
<i>a</i> /Å	8.18160(10)	8.18380(10)	8.18600(10)	8.18820(10)	8.19110(10)	8.1653(2)
<i>b</i> /Å	8.85370(10)	8.84960(10)	8.84680(10)	8.84520(10)	8.84810(10)	8.8929(2)
<i>c</i> /Å	11.3600(2)	11.3819(2)	11.40590(10)	11.43180(10)	11.4585(2)	11.2602(2)
α°	92.3840(10)	92.3840(10)	92.3810(10)	92.3760(10)	92.3430(10)	92.3270(10)
β°	107.7050(10)	107.7400(10)	107.7820(10)	107.8370(10)	107.9500(10)	107.6390(10)
γ°	95.2330(10)	95.1600(10)	95.0890(10)	95.0180(10)	94.9570(10)	95.6630(10)
Volume/Å ³	778.558(19)	779.865(19)	781.397(15)	783.107(15)	785.086(19)	773.25(3)
<i>Z</i>	2	2	2	2	2	2
$\rho_{\text{calc}}/\text{cm}^3$	1.551	1.549	1.546	1.542	1.538	1.562
μ/mm^{-1}	1.598	1.596	1.593	1.589	1.585	1.609
F(000)	372	372	372	372	372	372
Crystal size/mm ³	0.249 × 0.132 × 0.085	0.249 × 0.132 × 0.085	0.250 × 0.132 × 0.085	0.251 × 0.132 × 0.085	0.251 × 0.132 × 0.085	0.246 × 0.131 × 0.086
Radiation	MoK α ($\lambda = 0.71073$)					
θ range for data collection/ $^{\circ}$	1.89 to 26.12	1.88 to 26.15	1.88 to 26.13	1.88 to 26.13	1.87 to 26.06	1.90 to 26.12
Index ranges	-10 ≤ <i>h</i> ≤ 9, -10 ≤ <i>k</i> ≤ 10, -14 ≤ <i>l</i> ≤ 14	-10 ≤ <i>h</i> ≤ 9, -10 ≤ <i>k</i> ≤ 10, -14 ≤ <i>l</i> ≤ 14	-10 ≤ <i>h</i> ≤ 9, -10 ≤ <i>k</i> ≤ 10, -14 ≤ <i>l</i> ≤ 14	-10 ≤ <i>h</i> ≤ 9, -10 ≤ <i>k</i> ≤ 10, -14 ≤ <i>l</i> ≤ 14	-10 ≤ <i>h</i> ≤ 9, -10 ≤ <i>k</i> ≤ 10, -14 ≤ <i>l</i> ≤ 14	-10 ≤ <i>h</i> ≤ 9, -11 ≤ <i>k</i> ≤ 10, -13 ≤ <i>l</i> ≤ 13
Reflections collected	10740	10791	10816	10836	10809	10658
Independent reflections	3086 [R _{int} = 0.0240, R _{sigma} = 0.0228]	3107 [R _{int} = 0.0244, R _{sigma} = 0.0229]	3109 [R _{int} = 0.0244, R _{sigma} = 0.0234]	3118 [R _{int} = 0.244, R _{sigma} = 0.0234]	3107 [R _{int} = 0.0263, R _{sigma} = 0.0252]	3067 [R _{int} = 0.0250, R _{sigma} = 0.0238]
Data/restraints/parameters	3086/0/203	3107/0/208	3109 /0/208	3118/0/208	3107/0/224	3067/0/119
Goodness-of-fit on F ²	1.043	1.060	1.062	1.043	1.065	1.067
Final R indexes [I>=2σ (I)]	R ₁ = 0.0242, wR ₂ = 0.0588	R ₁ = 0.0250, wR ₂ = 0.0628	R ₁ = 0.0266, wR ₂ = 0.0645	R ₁ = 0.0281, wR ₂ = 0.0694	R ₁ = 0.0309, wR ₂ = 0.0746	R ₁ = 0.0224, wR ₂ = 0.0538
Final R indexes [all data]	R ₁ = 0.0263, wR ₂ = 0.0596	R ₁ = 0.0276, wR ₂ = 0.0640	R ₁ = 0.0299, wR ₂ = 0.0662	R ₁ = 0.0314, wR ₂ = 0.0710	R ₁ = 0.0346, wR ₂ = 0.0764	R ₁ = 0.0248, wR ₂ = 0.0548
Largest diff. peak/hole / e Å ⁻³	0.362/-0.199	0.404/-0.223	0.475/-0.233	0.532/-0.241	0.596/-0.266	0.315/-0.220
Mosaicity/°	0.39	0.39	0.39	0.39	0.39	0.39

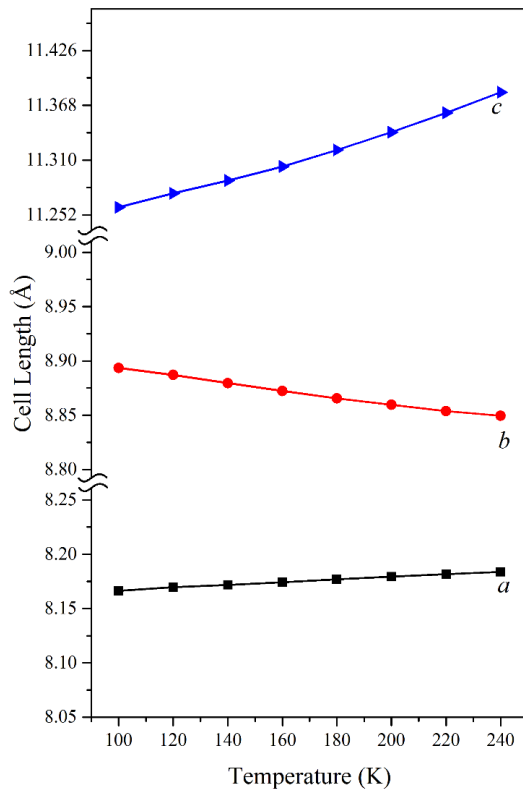


Figure S14 Variation of unit cell axes of **1** (including error bars) with temperature.

Table S9 Unit cell axes at variable temperatures for **1**.

T (K)	a (Å)	St. dev.*	b (Å)	St. dev.*	c (Å)	St. dev. *	Crystal mosaicity
100	8.1663	0.0002	8.8936	0.0002	11.2600	0.0002	0.39°
120	8.1696	0.0001	8.8871	0.0002	11.2748	0.0002	0.39°
140	8.1718	0.0001	8.8796	0.0002	11.2884	0.0002	0.40°
160	8.1742	0.0001	8.8724	0.0002	11.3032	0.0002	0.40°
180	8.1769	0.0001	8.8656	0.0001	11.3207	0.0002	0.40°
200	8.1794	0.0001	8.8596	0.0001	11.3396	0.0002	0.39°
220	8.1816	0.0001	8.8537	0.0001	11.3600	0.0002	0.39°
240	8.1838	0.0001	8.8496	0.0001	11.3819	0.0002	0.39°
260	8.1860	0.0001	8.8468	0.0001	11.4059	0.0001	0.39°
280	8.1882	0.0001	8.8452	0.0001	11.4318	0.0001	0.39°
298	8.1911	0.0001	8.8481	0.0001	11.4585	0.0002	0.39°
100-R	8.1653	0.0002	8.8929	0.0002	11.2602	0.0002	0.39°

*Standard deviation calculated from unit cell refinement using the Apex II software suite.

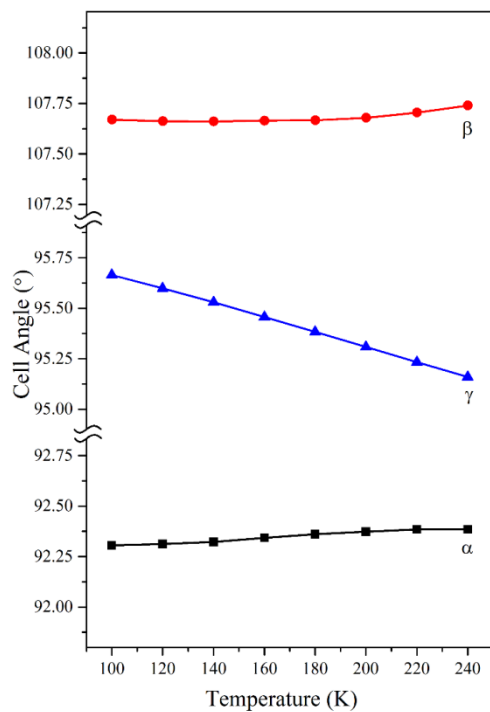


Figure S15 Variation of unit cell angles of **1** (including error bars) with temperature.

Table S10 Unit cell angles and volume at variable temperatures for **1**.

T (K)	α (°)	St. dev.*	β (°)	St. dev.*	γ (°)	St. dev. *	V(Å³)	St. dev. *	Crystal mosaicity
100	92.305	0.001	107.67	0.001	95.665	0.001	773.27	0.03	0.39°
120	92.312	0.001	107.662	0.001	95.599	0.001	774.17	0.02	0.39°
140	92.322	0.001	107.661	0.001	95.53	0.001	774.77	0.02	0.40°
160	92.343	0.001	107.665	0.001	95.457	0.001	775.46	0.02	0.40°
180	92.361	0.001	107.667	0.001	95.383	0.001	776.416	0.019	0.40°
200	92.373	0.001	107.679	0.001	95.309	0.001	777.476	0.019	0.39°
220	92.384	0.001	107.705	0.001	95.233	0.001	778.558	0.019	0.39°
240	92.384	0.001	107.74	0.001	95.16	0.001	779.865	0.019	0.39°
260	92.381	0.001	107.782	0.001	95.089	0.001	781.397	0.015	0.39°
280	92.376	0.001	107.837	0.001	95.018	0.001	783.107	0.015	0.39°
298	92.343	0.001	107.95	0.001	94.957	0.001	785.086	0.019	0.39°
100-R	92.327	0.001	107.639	0.001	95.663	0.001	773.25	0.03	0.39°

*Standard deviation calculated from unit cell refinement using the Apex II software suite.

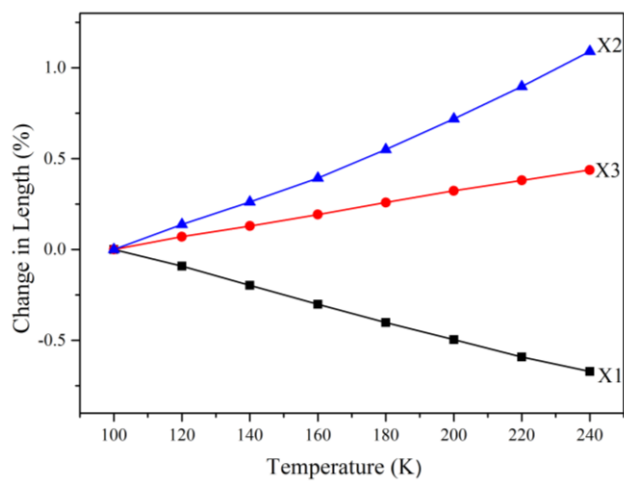


Figure S16 Plot of changes in principal axis lengths with increasing temperature for **1**.

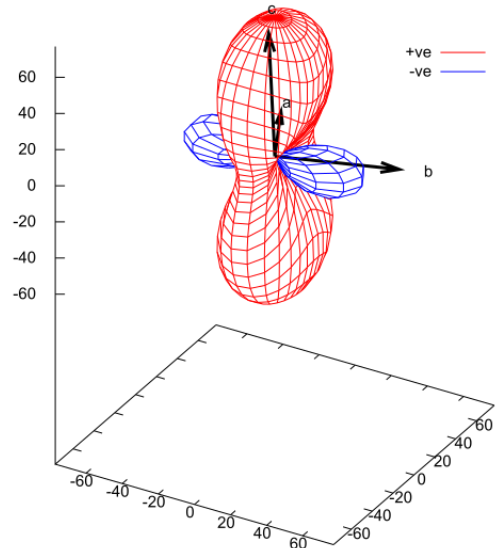


Figure S17 PASCal expansivity tensor plot for **1**.

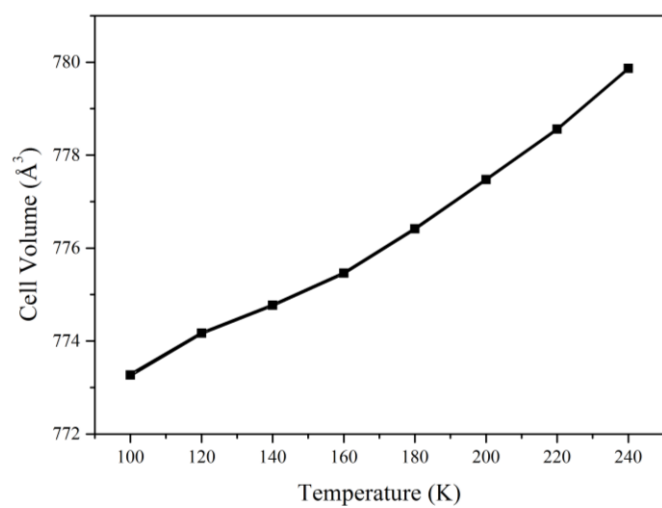


Figure S18 Variation of unit cell volume of **1** (including error bars) with temperature.

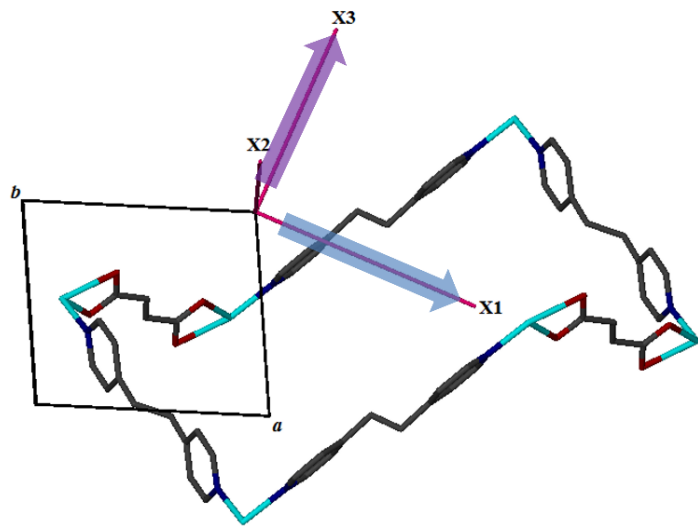


Figure S19 The orthogonal directions of the principal axes, X1 (NTE) and X3 (PTE) projected onto the crystallographic *ab* plane of **1**.

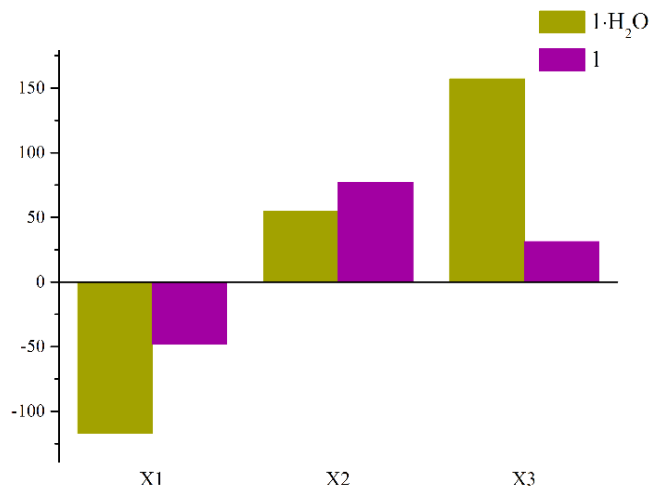


Figure 20 Plot showing variation of linear thermal expansion coefficients in **1·H₂O** and **1**.

Table S11 Selected bond angles at variable temperatures for **1**.

T (K)	O1–Zn1–N1 (°)	O1–Zn1–O3 (°)	O3–Zn1–N1 (°)	N1–Zn1–N2 (°)	O3–Zn1–N2 (°)	O1–Zn1–N2 (°)
100	108.19(5)	153.58(5)	95.27(5)	95.70(6)	96.45(5)	93.20(5)
120	108.27(5)	153.41(5)	95.32(5)	95.71(6)	96.64(5)	93.12(5)
140	108.34(5)	153.24(5)	95.45(5)	95.74(5)	96.71(5)	93.01(5)
160	108.43(5)	153.02(5)	95.54(5)	95.74(6)	96.84(5)	92.98(5)
180	108.40(5)	152.96(6)	95.60(5)	95.77(6)	96.93(5)	92.95(5)
200	108.47(5)	152.70(6)	95.73(5)	95.81(6)	97.06(5)	92.95(5)
220	108.51(6)	152.49(6)	95.85(6)	95.88(6)	97.27(6)	92.86(6)
240	108.63(6)	152.33(7)	95.85(6)	95.98(6)	97.40(6)	92.78(6)
260	108.73(7)	152.03(7)	95.98(6)	96.00(7)	97.59(6)	92.76(6)
280	108.86(7)	151.61(8)	96.13(7)	96.13(7)	97.87(7)	92.77(7)
298	108.95(8)	151.27(8)	96.27(8)	96.25(8)	98.15(8)	92.68(8)

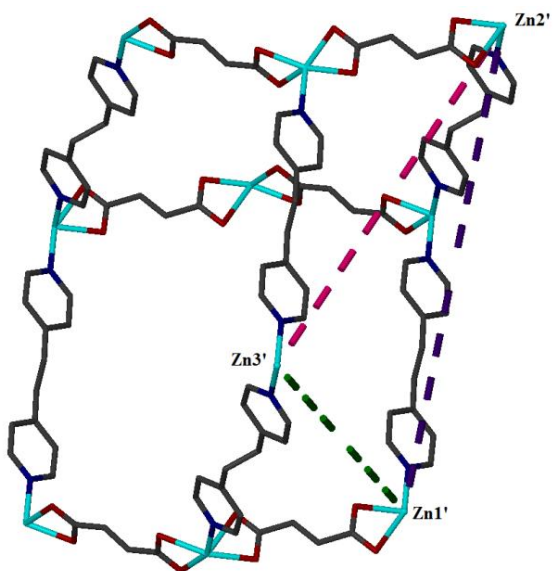


Figure S21 View of selected non-bonding distances within a single diamondoid network in **1**.

Table S12 List of selected non-bonding distances (in Å) within a single diamondoid network at variable temperatures for **1**.

T (K)	Zn1'....Zn2' [0 2 1]	Zn2'....Zn3' [-1 2 0]	Zn1'....Zn3' [1 0 -1]
100	20.6655(5)	18.8254(5)	15.7892(4)
120	20.6609(5)	18.8237(4)	15.8037(4)
140	20.6536(5)	18.8201(5)	15.8170(4)
160	20.6456(5)	18.8177(5)	15.8321(4)
180	20.6410(4)	18.8163(3)	15.8495(4)
200	20.6378(4)	18.8163(3)	15.8689(4)
220	20.6365(4)	18.8166(3)	15.8908(4)
240	20.6410(4)	18.8197(3)	15.9150(4)
260	20.6492(4)	18.8249(3)	15.9416(4)
280	20.6608(4)	18.8323(4)	15.9711(4)
298	20.6851(4)	18.8467(4)	16.0076(4)

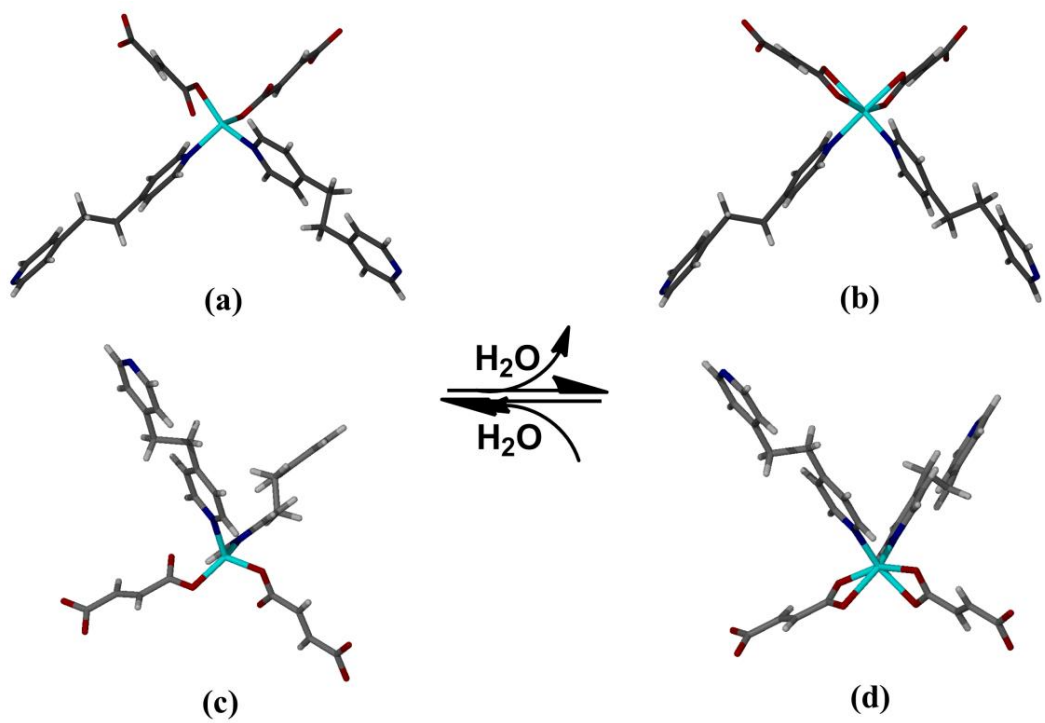


Figure 22 Conformational changes in BPA (a,b) and FMA (c,d) upon dehydration/rehydration.

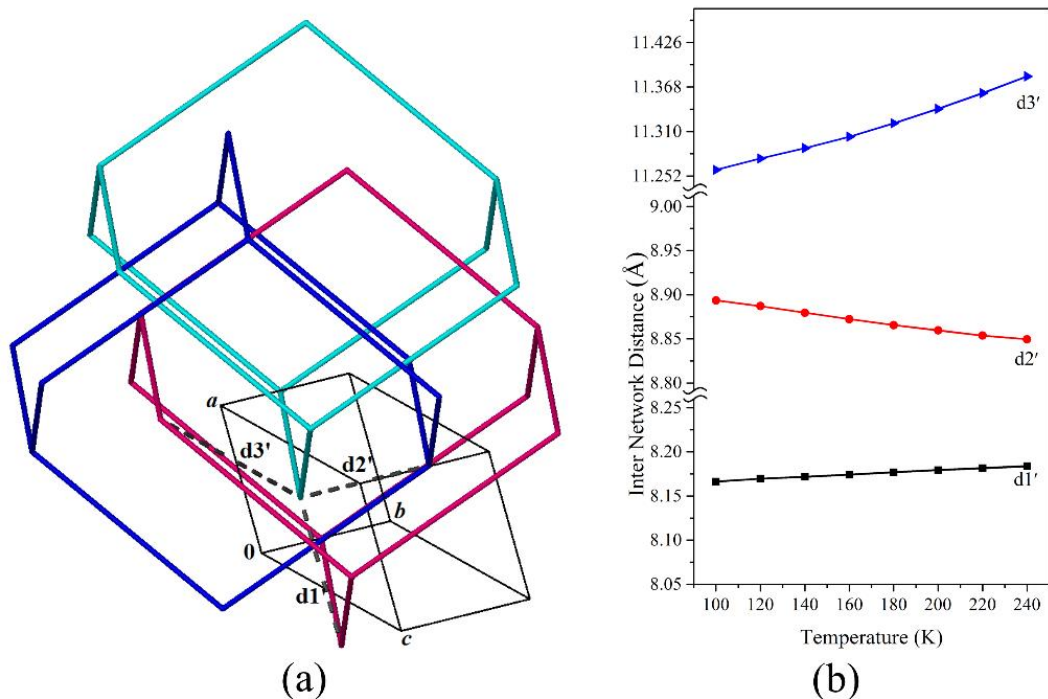


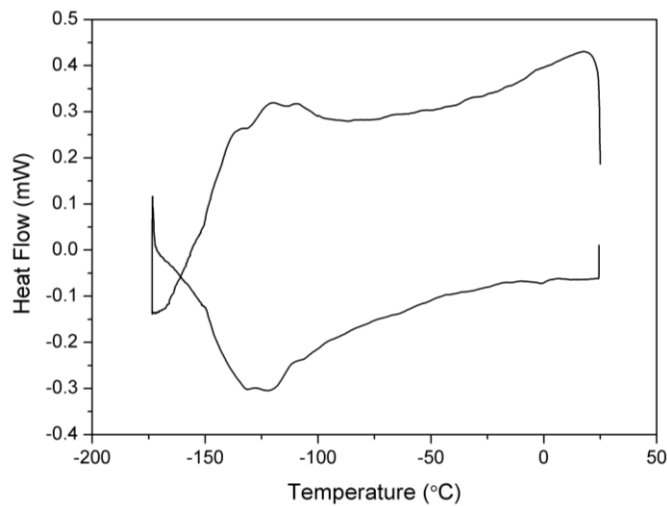
Figure S23 (a) Perspective view of various inter-network distances along the crystallographic axes (only three interpenetrated networks are shown for clarity) and (b) changes in the inter network distances with temperature in the case of **1**.

Table S13 List of selected inter diamondoid network distances at variable temperatures for **1**.

T (K)	d1' (Å)	d2' (Å)	d3' (Å)
100	8.1663(3)	8.8936(3)	11.2600(3)
120	8.1696(3)	8.8871(3)	11.2748(3)
140	8.1718(3)	8.8796(3)	11.2884(3)
160	8.1742(3)	8.8724(3)	11.3032(3)
180	8.1769(3)	8.8656(3)	11.3207(3)
200	8.1794(3)	8.8596(3)	11.3396(3)
220	8.1816(4)	8.8537(3)	11.3600(4)
240	8.1838(4)	8.8496(3)	11.3819(4)
260	8.1860(4)	8.8468(3)	11.4059(3)
280	8.1882(4)	8.8452(4)	11.4318(4)
298	8.1911(4)	8.8481(4)	11.4585(4)

Differential scanning calorimetry analysis

Differential scanning calorimetry (DSC) was carried out at a cooling rate of 5 °C min⁻¹ in the temperature range of 100-298 K, under a nitrogen flow of 50 mL min⁻¹ on a DSC Q100 instrument. 3-5 mg of sample was placed in an aluminium pan with a lid. An empty sealed pan was used as a reference.



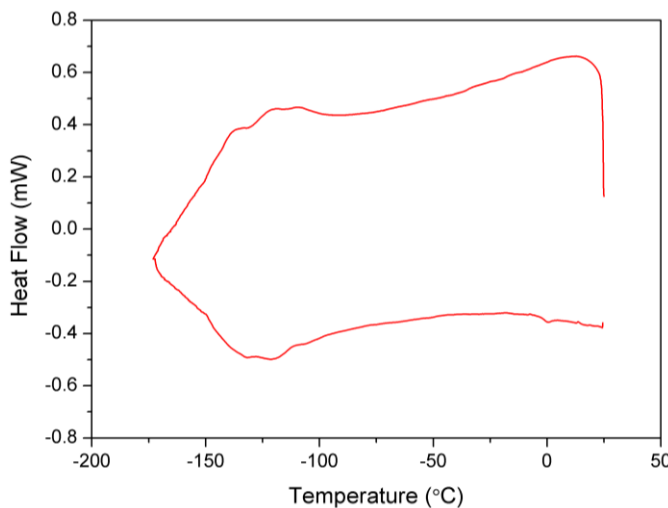


Figure 24 Differential scanning calorimetric thermogram of **1·H₂O** (top) and **1** (bottom).

Table S14 Single crystal data for 1_act and 1_rehydrated

Identification code	1_act	1_rehydrated
Empirical formula	C ₁₆ H ₁₄ N ₂ O ₄ Zn	C ₁₆ H ₁₆ N ₂ O ₅ Zn
Formula weight	363.66	381.68
Temperature/K	247(2)	100(2)
Crystal system	Triclinic	triclinic
Space group	P-1	P-1
a/Å	8.1801(19)	8.385(3)
b/Å	8.831(2)	9.210(3)
c/Å	11.441(3)	11.159(4)
α/°	92.396(2)	90.459(4)
β/°	107.797(2)	110.476(4)
γ/°	94.950(3)	100.507(5)
Volume/Å ³	782.0(3)	791.4(5)
Z	2	2
ρ _{calc} g/cm ³	1.544	1.602
μ/mm ⁻¹	1.591	1.581
F(000)	372.0	392.0
Crystal size/mm ³	0.33 × 0.14 × 0.08	0.33 × 0.13 × 0.1
Radiation	MoKα (λ = 0.71073)	MoKα (λ = 0.71073)
θ range for data collection/°	3.74 to 51.86	3.9 to 51.82
Index ranges	-6 ≤ h ≤ 10, -9 ≤ k ≤ 10, -13 ≤ l ≤ 14	-9 ≤ h ≤ 10, -7 ≤ k ≤ 11, -13 ≤ l ≤ 13
Reflections collected	4385	4403
Independent reflections	2989 [R _{int} = 0.0264, R _{sigma} = 0.0540]	3026 [R _{int} = 0.0292, R _{sigma} = 0.0623]
Data/restraints/parameters	2989/0/208	3026/0/226
Goodness-of-fit on F ²	1.050	1.026
Final R indexes [I>=2σ (I)]	R ₁ = 0.0440, wR ₂ = 0.0913	R ₁ = 0.0514, wR ₂ = 0.1248
Final R indexes [all data]	R ₁ = 0.0577, wR ₂ = 0.1005	R ₁ = 0.0673, wR ₂ = 0.1353
Largest diff. peak/hole / e Å ⁻³	0.395/-0.44	1.12/-0.62

Single-crystal to single-crystal transformation (SC-SC)

A small batch of **1·H₂O** crystals was activated at 100 °C overnight. A suitable crystal was selected from this batch and the single-crystal data were collected. These crystals were again immersed in water for 24 h, followed by SCXRD data collection on a single crystal that showed the reversal from **1** to **1·H₂O**. It is noteworthy that no apparent loss in crystal singularity was observed during dehydration/rehydration process. The crystals of **1** are not soluble in water.

References:

1. (a) Hocking, R. K.; Hambley, T. W. *Dalton Trans.* **2005**, 969-978; (b) Orpen, A. G.; Brammer, L. J. *Chem. Soc. Dalton Trans.* **1989**.
2. SAINT Data Reduction Software, Version 6.45; Bruker AXS Inc., Madison, WI, 2003.
3. (a) SADABS, Version 2.05; Bruker AXS Inc., Madison, WI, 2002; (b) Blessing, R. H. *Acta Crystallogr., Sect. A: Found. Crystallogr.* **1995**, *51*, 33–38.
4. Sheldrick, G. M. *Acta Crystallogr., Sect. A: Found. Crystallogr.* **2008**, *64*, 112–122.
5. Barbour, L. J. *J. Supramol. Chem.* **2001**, *1*, 189–191.